Available online at www.sciencedirect.com
ScienceDirect
Journal of the European Ceramic Society 31 (2011) 2277–2284
www.elsevier.com/locate/jeurceramsoc

Microstructure and mechanical properties of alumina ceramics reinforced by boron nitride nanotubes

Wei-Li Wang[a,b], Jian-Qiang Bi[a,b,*], Shou-Ren Wang[c], Kang-Ning Sun[a,b], Ming Du[a,b], Na-Na Long[a,b], Yu-Jun Bai[a,**]

[a] *Key Laboratory for Liquid-Solid Structural Evolution and Processing of Materials, Ministry of Education, Shandong University, Jinan 250061, PR China*
[b] *Engineering Ceramics Key Laboratory of Shandong Province, Shandong University, Jinan 250061, PR China*
[c] *School of Mechanical Engineering, University of Jinan, Jinan 250022, PR China*

Received 23 February 2011; received in revised form 17 May 2011; accepted 30 May 2011
Available online 25 June 2011

Abstract

Boron nitride nanotubes (BNNTs)/alumina composites were fabricated by hot pressing. The mechanical properties of the composites are greatly dependent upon the content of BNNTs. In comparison with monolithic alumina, the incorporation of BNNTs results in the improvement of bending strength and fracture toughness owing to the effective inhibition of grain growth. A routine toughening mechanism, especially the bridging of BNNTs at grain boundaries and the sufficient physical bonding between BNNTs and alumina matrix, is dominantly responsible for the increase in mechanical properties.

Keywords: Hot pressing; Composites; Mechanical properties; Al_2O_3; Boron nitride nanotubes

1. Introduction

Boron nitride (BN) has many excellent properties, such as low density, high thermal conductivity, stability and mechanical performances.[1] The similarity in structure makes BN a good substitute for carbon-related materials in lots of applications. BNNTs, a new form of BN focused in recent years,[2–5] are chemically and thermally stable compared to carbon nanotubes (CNTs).[6–8] Generally, CNTs readily oxidize above 400 °C in air,[9,10] and reactions may occur when CNTs are used as strengthening agent in composites of some metals (such as Fe, Ti, Cr and Zr) and their oxides, leading to partial or total loss of strengthening and toughening effect. In contrast, BNNTs are still stable in air at 800 °C, even at higher temperatures.[11] The tensile strength and Young's modulus of BNNTs are ∼30 GPa and ∼900 GPa, respectively, by measuring the applied forces and tube lengths until the nanotubes break.[12] The superior properties of BNNTs make them attractive in reinforcing composites especially the ceramic matrix composites.

Alumina (Al_2O_3) is one of the most widely used engineering ceramics, but the brittleness restricts its practical and potential applications as structural materials. Up to now, some attempts have been made to toughen and reinforce Al_2O_3 ceramic by CNTs. However, only few improvements were achieved.[13–15] In most of the attempts, no increase or even decrease in bending strength and fracture toughness occurred.[16–20] Associating with the extraordinary properties of CNTs, such results were disappointing. To date, only a few researches tried to increase the mechanical properties of ceramics and polymers by incorporating BNNTs. The strength and fracture toughness of barium calcium aluminosilicate glass composites reinforced with 4 wt.% of BNNTs could be increased by 90% and 35%, respectively.[21,22] The high-temperature superplasticity of Al_2O_3 and Si_3N_4 ceramics were enhanced by introducing 0.5 wt.% of BNNTs.[23] The elastic modulus of the BNNTs/polystyrene composites films was increased by ∼21%,[24] while that of the polymethyl methacrylate/BNNTs composites was increased by 19%, and the thermal conductivity was increased by three times.[25] Meanwhile, a drastically improved thermal conduc-

* Corresponding author at: Key Laboratory for Liquid-Solid Structural Evolution and Processing of Materials, Ministry of Education, Shandong University, Jinan 250061, PR China. Tel.: +86 531 88392439; fax: +86 531 88392315.
** Corresponding author. Tel.: +86 531 88392439; fax: +86 531 88392315.
E-mail addresses: bjq1969@163.com (J.-Q. Bi), byj97@126.com (Y.-J. Bai).

0955-2219/$ – see front matter. Crown Copyright © 2011 Published by Elsevier Ltd. All rights reserved.
doi:10.1016/j.jeurceramsoc.2011.05.042

tivity (∼270%) was achieved in polyvinyl alcohol polymeric composites containing catechin-modified-BNNT.[26] However, to the best of our knowledge, there is no research concerning the mechanical properties of BNNTs/Al_2O_3 composites at ambient temperature. In contrast to CNTs-reinforced composites, the investigations on BNNTs composites are remarkably inadequate due to the extreme difficulty in preparing highly pure BNNTs with a yield high enough to fabricate composites for tests.[27] Though several approaches have been proposed so far to synthesize BNNTs,[28–34] large-scale synthesis is still a challenge.

Recently, we developed a method to prepare BNNTs in large scale using CNTs as template,[35] providing more chances for further investigating the properties and applications of BNNTs. Followed by the large-scale preparation, we fabricated BNNTs/Al_2O_3 composites and studied the influence of BNNTs on the mechanical properties of Al_2O_3 ceramic at ambient temperature.

2. Experimental

The synthesis of BNNTs is the same as that reported in our previous work.[35] High-purity, micrometer-sized γ-Al_2O_3 powder was selected as raw material. The Al_2O_3 powder and BNNTs were mixed in ethanol by using Al_2O_3 milling balls with a ball-charge weight ratio of 7:1. The milling time is 8 h at a rotation rate of 300 rpm.

After drying, the mixtures were screened in a 100-mesh sieve. Then the mixtures were placed into a graphite die with a diameter of 42 mm, and hot pressed at 1500 °C in a multipurpose high-temperature furnace (Fujidenpa Kogyo Co., Ltd., Osaka, Japan) under a pressure of 25 MPa in argon atmosphere for 1 h. The BNNTs added to the composites were 0, 0.5, 1.0, 1.5, 2.0, 5.0 and 10.0 wt.%, respectively. The sintered samples were machined into rectangular specimens of 3.0 mm × 4.0 mm × 25 mm in size for bending strength measurement, and four specimens for each sample were tested by three-point bending test at a speed of 0.5 mm/min. In addition, fracture toughness of four specimens with the size of 2.0 mm × 4.0 mm × 25 mm for each sample was measured by single-edge notched beam (SENB) method. A notch of 2.0 mm in depth and width was cut in the middle of each specimen using thin diamond blade. The test was conducted by three-point bending at a speed of 0.05 mm/min on the same jig used for measuring the bending strength. Before testing, the edges of the bars were polished to form circular arc in order to reduce stress concentration. Both the bending strength and fracture toughness tests were conducted on a CMT5105 electromechanical universal testing machine (Shenzhen SANS Testing Machine Co., Ltd.) with a span length of 20 mm.

Moreover, the bulk density of the samples was measured by the Archimedes method in distilled water, where the theoretical densities for Al_2O_3 and BNNTs were 3.97 and 1.38 g/cm^3,[36] respectively. After polished, all the samples were thermally etched for 30 min at 1400 °C in a muffle furnace for grain size determination.

The morphology of BNNTs and the fracture surfaces of the composites were examined via a SU-70 type thermal field emission scanning electron microscope (FESEM). A JEOL JEM-2100 high-resolution transmission electron microscope (HRTEM) was used to characterize the pristine BNNTs and to investigate the microstructure and bonding between BNNTs and Al_2O_3 matrix by grinding the composites into powders.

Table 1
Relative density and grain size of samples.

BNNT content(wt.%)	Relative density (%)	Mean grain size (μm)
0	99.8	∼15
0.5	99.8	∼10
1.0	99.4	7
1.5	98.9	5
2.0	98.7	3
5.0	97.7	2
10.0	96.7	0.9

3. Results and discussion

The pristine BNNTs and those ball-milled with Al_2O_3 powders were examined by FESEM and HRTEM. Fig. 1a displays the morphology and surface features of the pristine BNNTs, whose diameters are all less than 100 nm and lengths up to several micrometers. The hollow structure and the walls of the nanotubes can be confirmed by HRTEM, as shown in the inset of Fig. 1a. After ball milling, BNNTs were well dispersed in Al_2O_3 powders, as displayed in Fig. 1b, and the nanotubes almost retain their original morphology.

The bending strength and fracture toughness of the BNNTs/Al_2O_3 composites were measured, and the average values of each sample were given as a function of BNNT content, as depicted in Fig. 2. It is clear that the mechanical properties are greatly dependent upon the amount of BNNTs in the composites. The composite containing 2.0 wt.% of BNNTs has the maximum bending strength of ∼532 MPa (Fig. 2a), which is increased by 67% compared to that of the pure Al_2O_3 ceramic (∼319 MPa). The composite with 1.0 wt.% of BNNTs exhibits the highest fracture toughness of ∼6.4 MPa m$^{1/2}$ (Fig. 2b), about 31% higher than that of the monolithic Al_2O_3 ceramic (∼4.9 MPa m$^{1/2}$). Meanwhile, the composite containing 2.0 wt.% of BNNTs possesses a high fracture toughness of ∼6.1 MPa m$^{1/2}$ as well, close to the highest one. The measurement result for fracture toughness depends on notch width, especially on the dispersion of BNNTs at the initiation site of crack propagation. Thus, within an appropriate scope for BNNTs content, it is probable that the fracture toughness is approximately the same. Additionally, because the notches of 2.0 mm in width is wider that those in literatures,[13,14,36,37] comparatively high toughness values were achieved due to the crack initiation at a blunt notch root. However, at least, the values can reflect the reinforcement effect arising from the incorporation of BNNTs.

Fig. 3 is the FESEM images to display the microstructures on polished, thermally etched samples. The monolithic Al_2O_3 exhibits a lot of large and uneven grains accompanying with a few tiny ones (Fig. 3a), while the composites have a smaller grain size (Fig. 3b–g). The mean grain size is summarized in Table 1. The distribution of grains is not uniform in the monolithic Al_2O_3

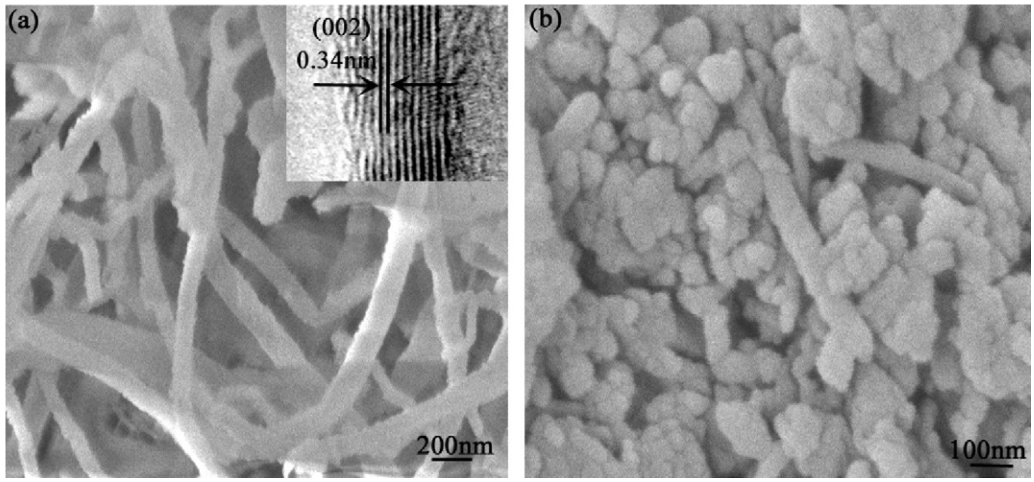

Fig. 1. FESEM images of the pristine BNNTs (a), and the BNNTs dispersed in Al_2O_3 powders (b). The inset in (a) is the lattice fringe image of BNNTs.

and the Al_2O_3 composite with 0.5 wt.% BNNT, so it is difficult to analyze the grain size accurately. The grain boundaries are clearly visible especially in the composites containing BNNTs due to the damage of BNNTs in the thermally etching process. Meanwhile, the addition of BNNTs changes the fracture mode as well (Fig. 4a and b), from edge and corner (corresponding to inter-granular fracture) to blurry and glaze-like feature (corresponding to trans-granular fracture).[39] In addition, most of the BNNTs distribute at grain boundaries, and a few within the grains. During sintering, the growth of Al_2O_3 particles adjacent to BNNTs gives rise to the incorporation of BNNTs into the grain boundaries or into the grains. The existence of BNNTs will depress the growth of Al_2O_3 particles into one large grain, resulting in an abrupt decrease in grain size. From Fig. 4c, the BNNTs encompassing an Al_2O_3 grain, as marked by arrow 1, could inhibit the abnormal grain growth efficiently just like what has happened in CNT-reinforced ceramics,[15,40] contributing to the increase in bending strength and fracture toughness of ceramics. What is more, the BNNTs attached to the grains at the junction can also strengthen the grain boundaries to bear more load. The modification of fracture mode is the powerful evidence for the strengthened grain boundaries arising from the incorporation of BNNTs. More details on the BNNTs at grain boundaries are shown in a higher magnification image (Fig. 4d), from which the BNNTs are flexible enough to follow the grain shape well at grain boundary. In particular, some imprints resulted from BNNTs can be clearly observed at grain boundaries on the fractured surface (Fig. 4e), as marked by the arrows. Additionally, some nano-sized clusters present in Fig. 4d–e, indicating a small part of nanotubes has been damaged probably during sintering. Besides the benefits from BNNTs, the accumulation of BNNTs at grain boundaries during sintering will depress the densification as well. Therefore, the relative density declines with increasing the BNNT content, as shown in Table 1.

Bridging and pullout are considered to be a major toughening mechanism for ceramics,[41] which may take effect during crack propagating and deflecting, and thus should be responsible for the increase in bending strength and fracture toughness of the BNNTs/Al_2O_3 composites. When crack propagates through the grain boundaries, BNNTs will become obstacles at first. With the propagation of crack, BNNTs across the crack will be stretched because their ends are fixed firmly in the grains, and they will fail when reaching their critical strain, thus will absorb lots of fracture energy,[38,42] leaving their ends in the grains.[43] The BNNTs paralleled to the propagation direction of crack will be peeled away from the matrix, also consuming some energy due to the

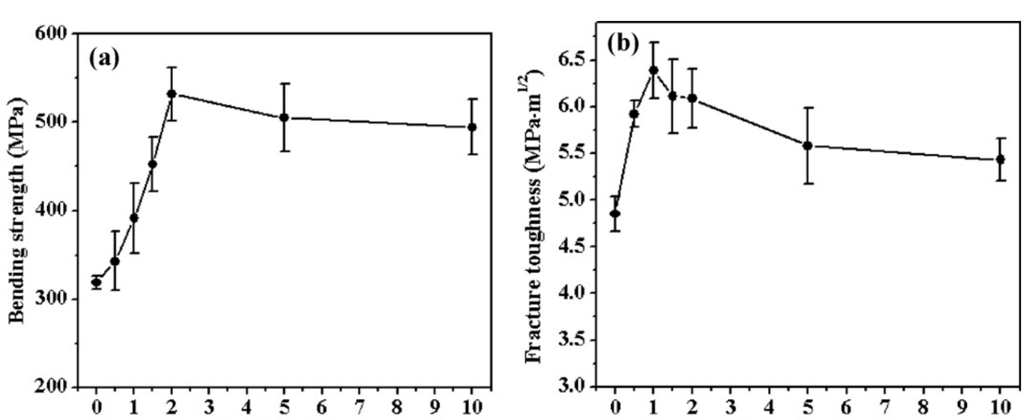

Fig. 2. Dependence of bending strength (a), and fracture toughness (b) on the amount of BNNTs in the composites.

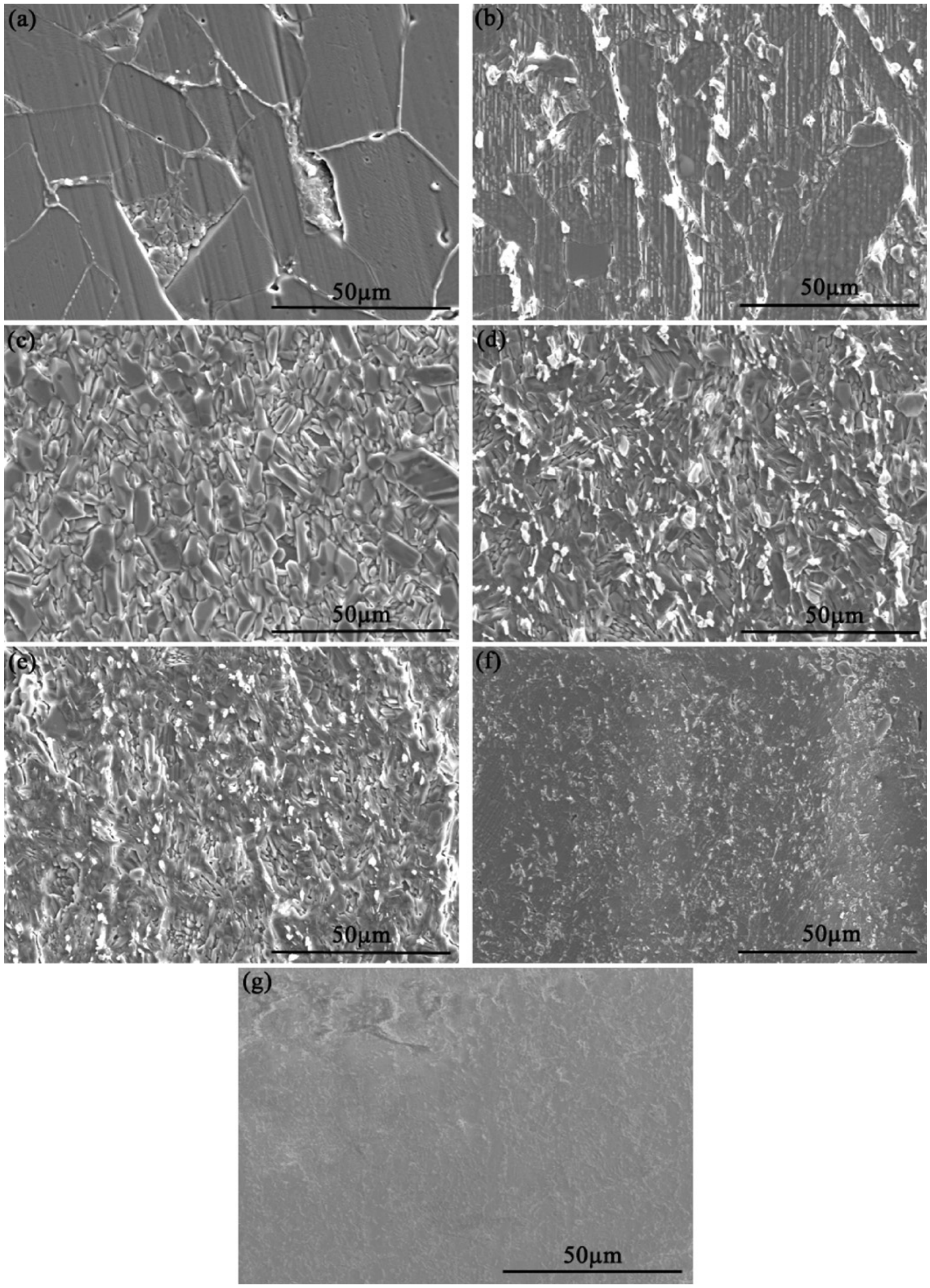

Fig. 3. FESEM images of thermally etched surfaces for monolithic Al_2O_3 (a), and the composites containing 0.5 wt.% (b), 1.0 wt.% (c), 1.5 wt.% (d), 2.0 wt.% (e), 5.0 wt.% (f), and 10.0 wt.% (g) BNNT.

friction between the BNNTs and the matrix. The FESEM image (Fig. 4f) of indentation-induced crack on the surface clearly demonstrates the bridging of BNNT (arrow 1), the fractured BNNT resulting from bridging failure (arrow 2) and the peeled BNNT from the matrix (arrow 3), indicative of the occurrence of a routine toughening mechanism.

Importantly, the coupling effect of grain interface bridging and nanotube bridging may take place in coarse-grained Al_2O_3 matrix, as proposed by Kim et al.[44] The coarse-grained matrix contains some active interface bridging which will induce nanotube bridging sufficiently. Fig. 4g clearly exhibits the occurrence of coupling effect of bridging, where the grain interface bridging (arrow 1) induces nanotube bridging (arrow 2). The BNNT becomes much thinner at the fractured location than other part of the nanotube, which is particularly true in Fig. 4h.

However, whether the pullout exists is still an issue. Xia et al. proposed that the pullout of nanotube was a major toughening mechanism in ceramic–matrix composite,[41] while Mukhopad-

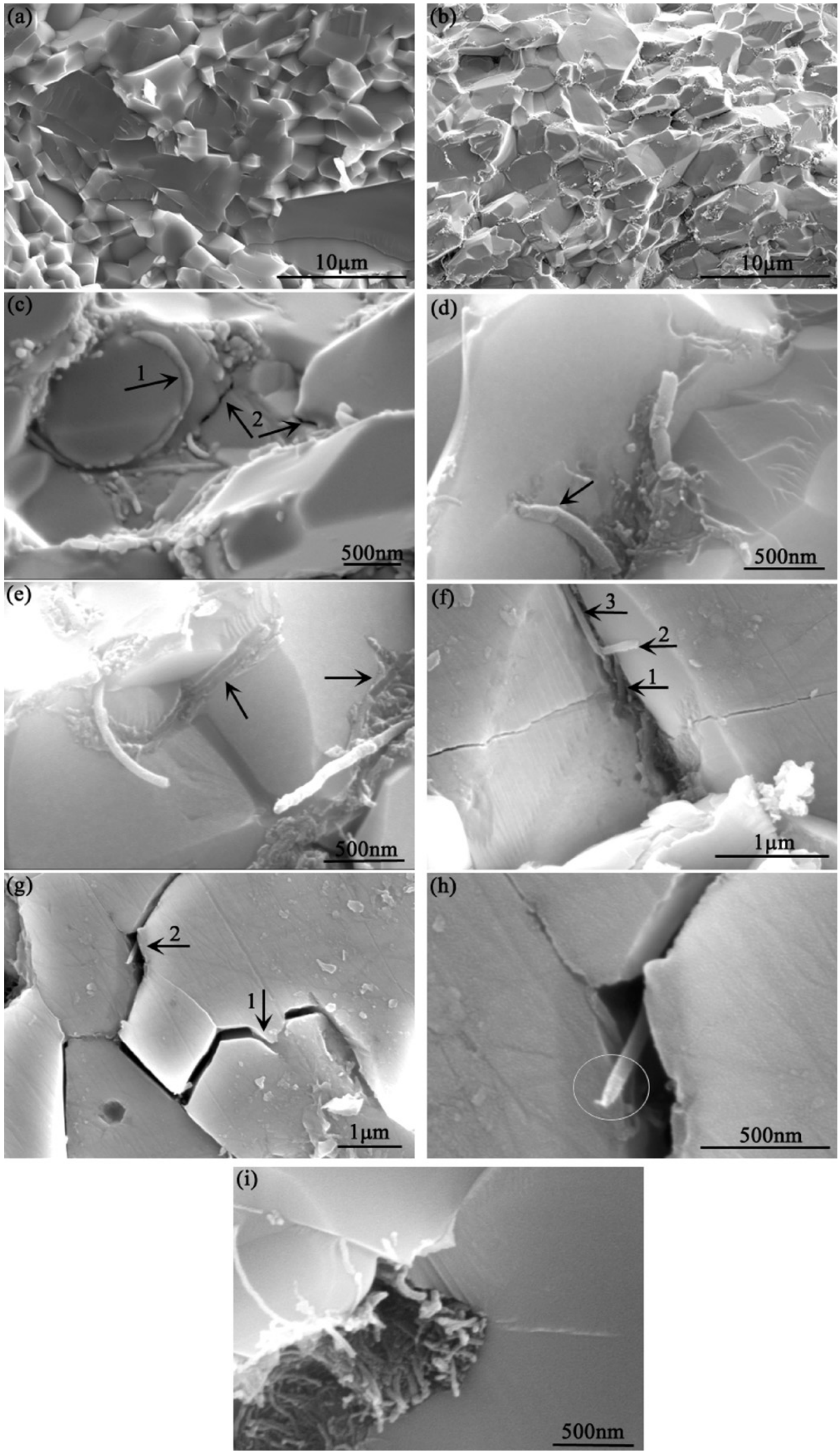

Fig. 4. FESEM images showing the crack and fracture surfaces of the samples containing 0 (a), 2.0 (b–h) and 10.0 wt.% (i) BNNT. (a) and (b) exhibit the modification of fracture mode from intergranular to transgranular fracture, (c) the BNNTs encompassing a Al_2O_3 grain, (d) and (e) the feature of BNNTs located at grain boundaries, (f)–(h) the nanotube bridging and coupling bridging, and (i) the agglomeration of BNNTs.

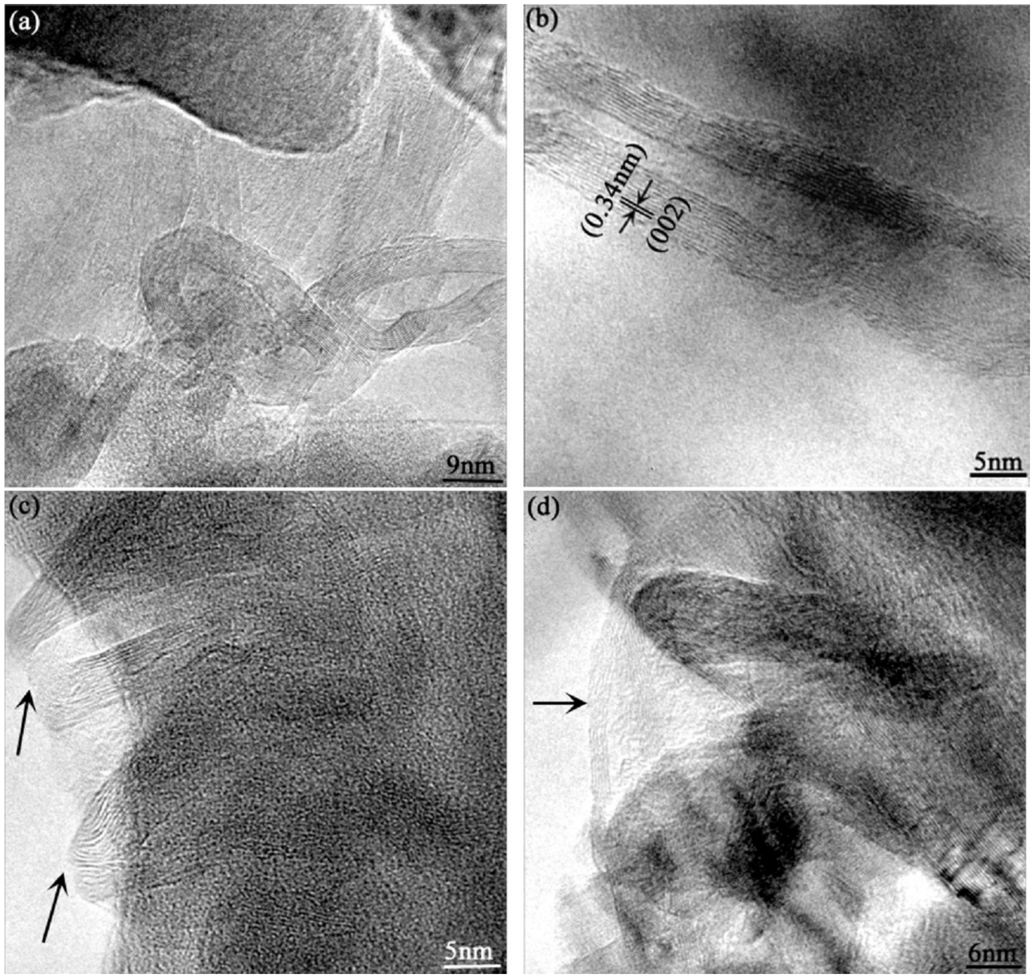

Fig. 5. HRTEM images of the composite containing 2.0 wt.% BNNT, displaying the morphology of BNNTs in the composite (a), at interface (b) and breakage sites (c and d).

hyay et al. evidenced that nanotubes were not similar to fibers in composite, and the pullout hardly occurred. Even if the phenomenon of nanotube pullout took place, the pullout length was very short.[45] We cannot determine accurately whether the residual length of BNNTs on the fractured surface is resulted from the BNNTs pullout or not. Nevertheless, the fracture of BNNTs indeed happens, which can dissipate energy during crack propagation.

According to literature, the coefficient of thermal expansion for α-Al_2O_3 and h-BN along *c*-axis direction is 8×10^{-6} and 40.5×10^{-6}/K, respectively, indicative of a large difference between them. So Si_3N_4 is sometimes added into BN/Al_2O_3 composites to form sialon phases for improving the bonding strength and for reducing thermal expansion.[46] The composites in this work exhibit excellent bending strength and fracture toughness. One of the key points is the absence of BNNT aggregation with a lower addition of BNNTs. However, some tiny cracks can be observed inside the composites due to the difference in coefficient of thermal expansion between BNNTs and Al_2O_3 matrix (arrow 2 in Fig. 4c). Unfortunately, excess addition of BNNTs is not propitious for densifying the BNNTs/Al_2O_3 composites, and the BNNT agglomeration may give rise to loose interfacial bonding and some defects, thus resulting in the decrease of mechanical properties. The aggregation of BNNTs in the matrix has no load-carrying ability, and produces a similar negative effect to pores.[13,47] Fig. 4i exhibits the BNNT agglomeration in the composite containing 10 wt.% of BNNTs, which will lead to the increase in porosity and the decrease in relative density of the composites, and eventually to the reduction of mechanical properties.

HRTEM examination was performed to acquire detailed information on fine microstructures. Similar to the flexible feature observed in FESEM, bended BNNTs are also examined by HRTEM (Fig. 5a). Meanwhile, BNNTs can be determined by the lattice fringe image in Fig. 5b where the lattice spacing of 0.34 nm corresponds to the (0 0 2) plane of h-BN. It is worth noting that the BNNTs at the breakage sites have an obvious tendency to thin down, as shown in Fig. 5c and d, demonstrating that the BNNTs subjected to a large strain before break, and thus contributes to improving strength and toughness. Furthermore, the bonding of BNNTs to the matrix is clearly displayed in Fig. 5b. The tightly bonding is favorable to improving the friction at interfaces and to forming bridging, and thus results in the increased mechanical properties.

Excellent interfacial strength is the guarantee for nanotube pullout and bridging. Generally, enhanced interfacial strength originates from physical and/or chemical effects induced residual thermal stress and/or chemical bonding between the matrix and the reinforcement phase. For CNTs-reinforced composites, both effects especially chemical bonding plays a vital role in improving the mechanical properties. Carbon is an active reductant at elevated temperatures, and the interfacial reactions could give rise to the detectable diffusion layer. Very recently, Ahmad et al. reported that a possible aluminium oxy-carbide generated by carbothermal reduction process during sintering CNTs/Al_2O_3 nanocomposites could act as the main interfacial phase.[39] For BNNTs-reinforced composites, BN is more chemically stable than carbon, and it is difficult to generate interfacial reactions, so the diffusion layer can hardly be detected as revealed in Fig. 5b. In addition, the residual thermal stress between Al_2O_3 and BNNTs can be calculated by the following equation:

$$\sigma = \int_{T}^{Ts} \frac{\Delta\alpha}{1/E_B + V_B/E_A V_A} dT \quad (1)$$

where σ is the residual stress; $\Delta\alpha$, the difference between the coefficient of thermal expansion of Al_2O_3 and BNNTs; E_A and E_B, Young's modulus of Al_2O_3 and BNNTs, respectively; V_A and V_B, the volume fraction of Al_2O_3 and BNNTs, respectively; T_s and T, the sintering point and room temperature, respectively. When the parameters are assigned as $\Delta\alpha = 32.5 \times 10^{-6}$/K, $E_B = 900$ GPa,[12] $E_A = 350$ GPa,[14] $V_B = 0.06$, $V_A = 0.94$, $T = 298$ K, and $T_s = 1773$ K, the σ value calculated by Eq. (1) is approximately 37 GPa. For calculating the volume fraction, the densities of Al_2O_3 and BNNTs are 3.97 and 1.38 g/cm^3,[36] respectively.

It is amazing that such a high residual thermal stress calculated did not lead to cracks in the composites. Actually, the residual thermal stress existing between Al_2O_3 and BNNTs is much less than that calculated, and the interfacial strength between nanotubes and matrix is weak compared to the fiber-reinforced polymer composites.[48] The main reason lies in the difference in Young's modulus of BNNTs prepared by various methods, also the modulus may change with raising temperature other than a constant. In our experiments, the Young's modulus of the as-obtained BNNTs cannot reach the reported value because of the defect-induced strength reduction in BNNTs.[12] What is more, the equation can only express the residual thermal stress roughly. Anyway, the existence of residual thermal stress is inevitable, but is not as large as the calculated value. As shown in Fig. 4c, the tiny cracks are indicative of the large residual thermal stress in the composites. The distinct difference in thermal expansion coefficient between the matrix and the reinforcement phase will result in compressive stress zone near interface, where the compressive stress around crack tip may decrease the crack length, and prohibit further generation and propagation of the cracks. As a consequence, the sufficient physical bonding in the composites is partly responsible for the improvement in strength and toughness.

4. Conclusions

In conclusion, the mechanical properties of hot pressed Al_2O_3 could be greatly improved by introducing BNNTs. Compared with the properties of monolithic Al_2O_3 ceramic, the composite containing 2.0 wt.% of BNNTs exhibits a bending strength increased by 67%, and that containing 1.0 wt.% of BNNTs has a fracture toughness increased by 31%. The addition of BNNTs greatly influences the grain size due to the effective inhibition of grain growth. In addition, the BNNTs at grain boundaries and the sufficient physical bonding between BNNTs and Al_2O_3 matrix lead to the bridging of nanotubes and the coupling effect of grain interface bridging and nanotube bridging, which are mainly responsible for the increase in mechanical properties. Therefore, BNNTs may be a promising and effective additive for reinforcing structural ceramics and other material systems.

Acknowledgements

This work is supported by the National Natural Science Foundation of China (Nos. 50872072, 51042005, and 50972076), Independent Innovation Foundation of Shandong University (2009TS001) and Graduate Independent Innovation Foundation of Shandong University (31370070613213).

References

1. Arya SPS, Amico AD. Preparation, properties and applications of boron nitride thin film. *Thin Solid Films* 1988;**157**:267–82.
2. Hamilton EJM, Dolan SE, Mann CM, Colijn HO, McDonald CA, Shore SG. Preparation of amorphous boron nitride and its conversion to a turbostratic, tubular form. *Science* 1993;**260**:659–61.
3. Chopra NG, Luyken RJ, Cherrey K, Crespi VH, Cohen ML, Louie SG, et al. Boron nitride nanotubes. *Science* 1995;**269**:966–7.
4. Blase X, Rubio A, Lohen SG. Stability and band gap constancy of boron nitride nanotubes. *Eur Phys Lett* 1994;**28**:335–40.
5. Chopra NG, Zettl A. Measurement of the elastic modulus of a multi-wall boron nitride nanotube. *Solid State Commun* 1998;**105**:297–300.
6. Vaccarini L, Goze C, Henrard L, Hernández E, Bernier P, Rubio A. Mechanical and electronic properties of carbon and boron-nitride nanotubes. *Carbon* 2000;**38**:1681–90.
7. Suryavanshi AP, Yu MF, Wen JG, Tang CC, Bando Y. Elastic modulus and resonance behavior of boron nitride nanotubes. *Appl Phys Lett* 2004;**84**:2527–9.
8. Chang CW, Han WQ, Zettl A. Thermal conductivity of B–C–N and BN nanotubes. *Appl Phys Lett* 2005;**86**:173102.
9. Chen Y, Zou J, Campbell SJ, Caer GL. Boron nitride nanotubes: pronounced resistance to oxidation. *Appl Phys Lett* 2004;**84**:2430–2.
10. Peigney A, Laurent Ch, Flahaut E, Rousset A. Carbon nanotubes in novel matrix nanocomposites. *Ceram Int* 2000;**26**:677–83.
11. Golberg D, Bando Y, Kurashima K, Sato T. Synthesis and characterization of ropes made of BN multiwalled nanotubes. *Scripta Mater* 2001;**44**:1561–5.
12. Wei X, Wang MS, Bando Y, Golberg D. Tensile tests on individual multiwalled boron nitride nanotubes. *Adv Mater* 2010;**2**:4895–9.
13. Yamamoto G, Omori M, Hashida T, Kimura H. A novel structure for carbon nanotube reinforced alumina composites with improved mechanical properties. *Nanotechnology* 2008;**19**:315708.
14. Fan JP, Zhuang DM, Zhao DQ, Zhang G, Wu MS. Toughening and reinforcing alumina matrix composite with single-wall carbon nanotubes. *Appl Phys Lett* 2006;**89**:121910.

15. Zhan GD, Kuntz JD, Wan J, Mukherjee AK. Single-wall carbon nanotubes as attractive toughening agents in alumina-based nanocomposites. *Nat Mater* 2003;**2**:38–42.
16. Peigney A, Laurent Ch, Dumortier O, Rousset A. Carbon nanotubes–Fe–alumina nanocomposites. Part I. Influence of the Fe content on the synthesis of powders. *J Eur Ceram Soc* 1998;**18**:1995–2004.
17. Laurent Ch, Peigney A, Dumortier O, Rousset A. Carbon nanotubes–Fe–alumina nanocomposites Part. II. Microstructure and mechanical properties of the hot-pressed composites. *J Eur Ceram Soc* 1998;**18**:2005–13.
18. Flahaut E, Peigney A, Laurent Ch, Marlière Ch, Chastel F, Rousset A. Carbon nanotube–metal-oxide nanocomposites: microstructure, electrical, conductivity and mechanical properties. *Acta Mater* 2000;**48**: 3803–12.
19. Sheldon BW, Curtin WA. Nanoceramic composites: tough to test. *Nat Mater* 2004;**3**:505–6.
20. Peigney A. Composite materials: tougher ceramics with nanotubes. *Nat Mater* 2003;**2**:15–6.
21. Choi SR, Bansal NP, Garg A. Mechanical and microstructure characterization of boron nitride nanotubes-reinforced SOFC seal glass composite. *Mater Sci Eng A* 2007;**460–461**:509–15.
22. Bansal NP, Hurst JB, Choi SR. Boron nitride nanotubes–reinforced glass composites. *J Am Ceram Soc* 2006;**89**:388–90.
23. Huang Q, Bando Y, Xu X, Nishimura T, Zhi C, Tang C, et al. Enhancing superplasticity of engineering ceramics by introducing BN nanotubes. *Nanotechnology* 2007;**18**:485706.
24. Zhi C, Bando Y, Tang C. Boron nitride nanotubes/polystyrene composites. *J Mater Res* 2006;**21**:2794–800.
25. Zhi CY, Bando Y, Wang WL, Tang CC, Kuwahara H, Golberg D. Mechanical and thermal properties of polymethyl methacrylate–BN nanotube composites. *J Nanomater* 2008;**2008**:642036.
26. Terao T, Bando Y, Mitome M, Zhi C, Tang C, Golberg D. Thermal conductivity improvement of polymer films by catechin-modified boron nitride nanotubes. *J Phys Chem C* 2009;**113**:13605–9.
27. Zhi C, Bando Y, Tang C, Honda S, Sato K, Kuwahara H, et al. Characteristics of boron nitride nanotube–polyaniline composites. *Angew Chem Int Ed* 2005;**44**:7929–32.
28. Loiseau A, Willaime F, Demoncy N, Hug G, Pascard H. Boron nitride nanotubes with reduced numbers of layers synthesized by arc discharge. *Phys Rev Lett* 1996;**76**:4737–40.
29. Guo T, Nikolaev P, Rinzler AG, Tomanek D, Colbert DT, Smalley RE. Self-assembly of tubular fullerenes. *J Phys Chem* 1995;**99**: 10694–7.
30. Lourie OR, Jones CR, Bartlett BM, Gibbons PC, Ruoff RS, Buhro WE. CVD growth of boron nitride nanotubes. *Chem Mater* 2000;**12**: 1808–10.
31. Golberg D, Bando Y, Tang C, Zhi C. Boron nitride nanotubes. *Adv Mater* 2007;**19**:2413–32.
32. Zhi C, Bando Y, Tang C, Golberg D. Boron nitride nanotubes. *Mater Sci Eng R* 2010;**70**:92–111.
33. Chen Y, Gerald JF, Williams JS, Bulcock S. Synthesis of boron nitride nanotubes at low temperatures using reactive ball milling. *Chem Phys Lett* 1999;**299**:260–4.
34. Bechelany M, Bernard S, Brioude A, Cornu D, Stadelmann P, Charcosset C, et al. Synthesis of boron nitride nanotubes by a template-assisted polymer thermolysis process. *J Phys Chem C* 2007;**111**:13378–84.
35. Bi JQ, Wang WL, Qi YX, Bai YJ, Pang LL, Zhu HL, et al. Large-scale synghesis BN nanotubes using carbon nanotubes as template. *Mater Lett* 2009;**63**:1299–302.
36. Zhi C, Bando Y, Tang C, Golberg D. Specific heat capacity and density of multi-walled boron nitride nanotubes by chemical vapor deposition. *Solid State Commun* 2011;**151**:183–6.
37. Fan J, Zhao D, Wu M, Xu Z, Song J. Preparation and microstructure of multi-wall carbon nanotubes toughened Al_2O_3 composites. *J Am Ceram Soc* 2006;**89**:750–3.
38. Ahmad I, Cao H, Chen H, Zhao H, Kennedy A, Zhu YQ. Carbon nanotube toughened aluminium oxide nanocomposite. *J Eur Ceram Soc* 2010;**30**:865–73.
39. Ahmad I, Unwin M, Cao H, Chen H, Zhao H, Kennedy A, et al. Multi-walled carbon nanotubes reinforced Al_2O_3 nanocomposites: mechanical properties and interfacial investigations. *Compos Sci Technol* 2010;**70**:1199–206.
40. Inam F, Yan H, Peijs T, Reece JM. The sintering and grain growth behaviour of ceramic–carbon nanotube nanocomposites. *Compos Sci Technol* 2010;**70**:947–52.
41. Xia Z, Riester L, Curtin WA, Li H, Sheldon BW, Liang J, et al. Direct observation of toughening mechanisms in carbon nanotube ceramic matrix composites. *Acta Mater* 2004;**52**:931–44.
42. Peigney A, Garcia FL, Estournès C, Weibel A, Laurent Ch. Toughening and hardening in double-walled carbon nanotube/nanostructured magnesia composites. *Carbon* 2010;**48**:1952–60.
43. Yamamoto G, Shirasu K, Hashida T, Takagi T, Suk JW, An J, et al. Nanotube fracture during the failure of carbon nanotube/alumina composites. *Carbon* 2011, doi:10.1016/j.carbon.2011.04.022.
44. Kim SW, Chung WS, Sohn KS, Son CY, Lee S. Improvement of flexural strength and fracture toughness in alumina matrix composites reinforced with carbon nanotubes. *Mater Sci Eng A* 2009;**517**:293–9.
45. Mukhopadhyay A, Chu BTT, Green MLH, Todd RI. Understanding the mechanical reinforcement of uniformly dispersed multiwalled carbon nanotubes in alumino-borosilicate glass ceramic. *Acta Mater* 2010;**58**:2685–97.
46. Li Y, Qiao G, Jin Z. Mechinable Al_2O_3/BN composite ceramics with strong mechanical properties. *Mater Res Bull* 2002;**37**:1401–9.
47. Yamamoto G, Omori M, Yokomizo K, Hashida T, Adachi K. Structural characterization and frictional properties of carbon nanotube/alumina composites prepared by precursor method. *Mater Sci Eng B* 2008;**148**:265–9.
48. Zhang T, Kumari L, Du GH, Li WZ, Wang QW, Balani K, et al. Mechanical properties of carbon nanotube–alumina nanocomposites synthesized by chemical vapor deposition and spark plasma sintering. *Compos Part A* 2009;**40**:86–93.